4-12-2019

Using Drone Acquired, High-Resolution, Multispectral Imaging to Predict and Monitor Coastal Dune Mobility: An Example from the Southeastern Shore of Lake Michigan

Jacob T. Stid
Hope College

USING DRONE ACQUIRED, HIGH-RESOLUTION, MULTISPECRAL IMAGING TO PREDICT AND MONITOR COASTAL DUNE MOBILITY: AN EXAMPLE FROM THE SOUTHEASTERN SHORE OF LAKE MICHIGAN

Jacob T. Stid[1], Brian Yurk[2], Edward Hansen[1], and Paul Pearson[2]

[1]Geological and Environmental Sciences Department, Hope College, Holland, Michigan, [2]Mathematics Department, Hope College, Holland, Michigan

INTRODUCTION

Sand dunes migrate downwind when they are covered with bare sand, but are anchored in place when covered by vegetation. Migrating dunes can cover and destroy buildings, fields, and parking lots. In the past, coastal dune management has focused on planting vegetation in order to stabilize dunes. More recently we have realized that some mobility is required for maintaining the ecological diversity of coastal dune complexes and the management focus has been shifting towards preventing over stabilization.

This poster is reporting on an ongoing study using drone-acquired, high-resolution, multispectral images to monitor and predict dune mobility in a 70 ha coastal dune preserve (Figure 1) at Saugatuck Harbor Natural Area (SHNA), on the southeastern shore of Lake Michigan. Dune grass is the dominant vegetation over this preserve which also contains several active blowouts and other patches of bare sand, as well as an interdunal wetland.

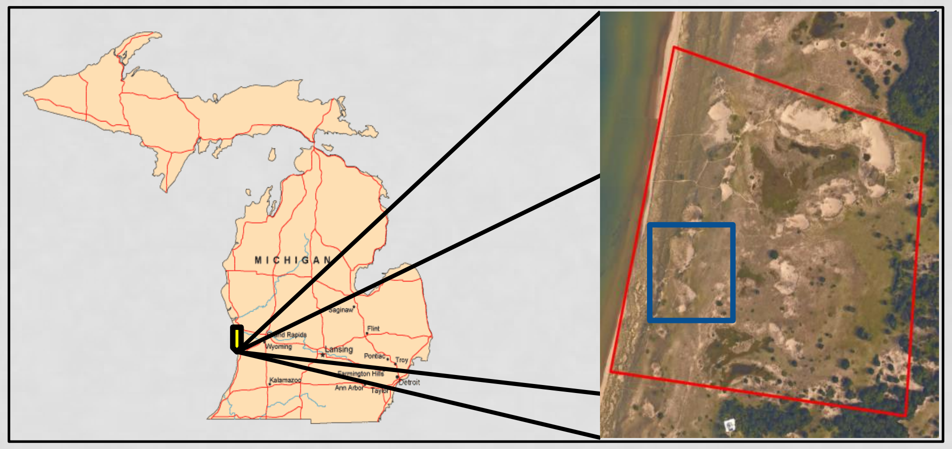

Figure 1: Map of Michigan with the location of Saugatuck Harbor Natural Area pinned and a larger satellite image showing the dune field examined. The red rectangle present in the satellite image shows the location of the study area. The blue rectangle denotes the location of the images used in this poster.

METHODS

Acquiring Drone Images

The Michigami Consulting Group of Holland, Michigan was contracted to conduct three drone flights (Figure 2) recording spectral and elevation data of a portion the SHNA preserve (Figures 1). On July 31st, 2017, a DJI Matrice M600 drone carrying a Canon converted camera recorded spectral imagery over the Near-Infrared (NIR), Red, and Green bands. On March 17th, 2018, a DJI Matrice M200 drone carrying an Red-Green-Blue (RGB) DJI X5S aerial camera mapped topography by parallax (Figure 3 and 4). On July 14th, 2018, a DJI Matrice M200 drone carrying a converted NDVI X4S aerial camera recorded spectral imagery again over the NIR, R, G bands. The images have a resolution of .87 cm by .87 cm.

Figure 2: The DJI Matrice M200 drone carrying the RGB DJI X5S aerial cameral flown on March 17th 2018.

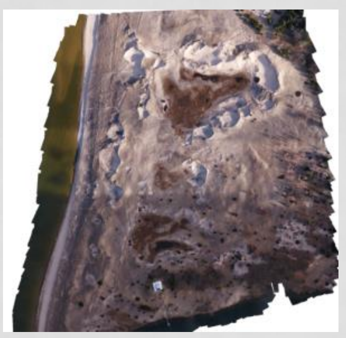

Figure 3: The RGB imagery of the March 17th, 2018 flight with the RGB DJI X5S aerial camera.

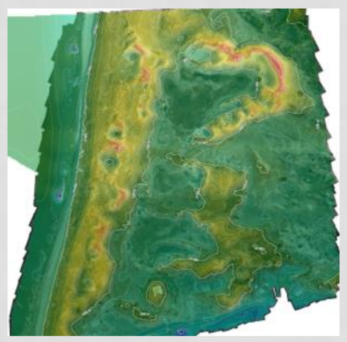

Figure 4: Elevation data deduced from RGB DJI X5S aerial topographic imagery.

NDVI METHOD

The normalized difference vegetation index (NDVI) is commonly used to deduce vegetation coverage using the near infrared and red spectral bands (NASA, 2017):

$$NDVI = \frac{NIR - Red}{NIR + Red}$$

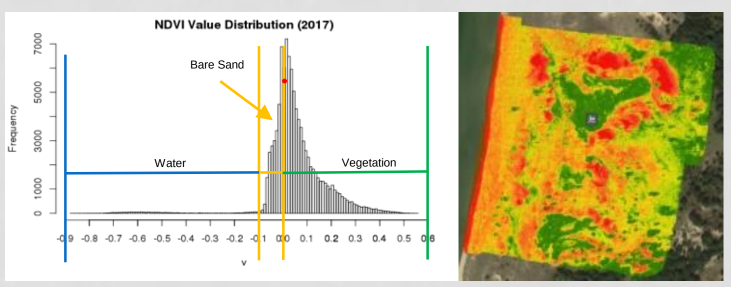

Figure 5: Spectral data from the flight on July 31st, 2017. The left image shows the ranges of values produced by the NDVI equation and the relative category ranges and the right image shows the NDVI values over the study area.

NDVI values can range from -1 to 1. By comparing NDVI values for specific areas covered with water, bare sand, or vegetation (Figure 5), NDVI values were assigned to each category: -1 to - 0.1 for water, -0.1 to 0 for bare sand, and 0 to 1 for vegetation.

DEFLATION MODEL

Wind Shadow Index

The wind shadow effect occurs in the lee slope of an obstacle such as a dune. Following Werner (1995), a wind shadow with minimal deflation extends at a 15º angle from the crest of the obstacle to the ground. Areas within the wind shadow were given a 0% probability of deflation while areas outside the shadow were given a 100% probability of deflation (Figures 6). Wind shadows were determined by applying a solar shadow function at a solar angle of 15 degrees to the horizon.

Slope Index

The steeper the slope in the windward direction, the more difficult it is to transport sand upslope and the easier it is to transport sand down slope. The effect of slope is given in Figures 7. In these diagrams, the probability of deflation ranged from 0.9 for the largest positive slopes to 1.0 for the largest negative slopes.

Vegetation (Proximal and Upwind) Index

NDVI values were used to classify each pixel as predominantly vegetation or water, or predominantly bare sand. The values were averaged to obtain the proportion of vegetated pixels in a sliding window of 5 x 5 pixels (total area of 19 cm^2) to form our proximal vegetation index. A threshold value of 20% vegetation coverage (Lancaster and Baas, 1998) was set as the limit above which sand grain transport was assumed to be negligible. The proximal vegetation deflation index was set to 0 for vegetation coverage above 20% and increased linearly to an index value of 100% in regions with between 20% and 0% vegetation coverage (Figure 8).

Vegetation upwind from a bare patch can dissipate wind energy decreasing the probability of deflation. A Gaussian sliding filter elongated in the upwind direction was applied to the vegetation data set to approximate the upwind vegetation of each cell. A 20% threshold value was set as the limit for deflation and the upwind deflation index (Figures 9) increased linearly from 0% (upwind vegetation coverage of 20%) to 100% (upwind vegetation coverage of 0%).

Elevation Index

Topographical acceleration at high elevations increases the winds ability to transport sand. This effect is illustrated in Figure 10. The elevation index ranged from an index value of 90% for the lowest elevations to 100% for the highest elevations.

Combination of indices

As a first approximation, the indices were combined in the same way as one would combine probabilities. The deflation potential combination is:

$$I_d = I_e \; x \; I_s \; x \; I_{ws} \; x \; (1 - [1 - I_{uv}][1 - I_p])$$

Where:

$I_d = Deflation\ Potential$
$I_e = Elevation\ Effect\ on\ Deflation\ Potential$
$I_s = Slope\ Effect\ on\ Deflation\ Potential$
$I_{ws} = Wind\ Shadow\ Effect\ on\ Deflation\ Potential$
$I_{uv} = Upwind\ Vegetation\ Effect\ on\ Deflation\ Potential$
$I_p = Proximal\ Vegetation\ Effect\ on\ Deflation\ Potential$

Separate maps of deflation potential were created for the 16 primary directions of the compass rose. Data from a nearby weather station were used to calculate the relative sand drift potential in each direction (Fryberger, 1979). Deflation potentials were combined proportionately to the sand drift potential in each direction to create an overall deflation potential map (Figure 11). This simple model will be tested and refined against observations of dune mobility over the next several years.

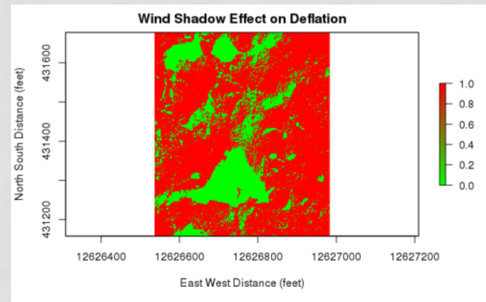

Figure 6: The wind shadow effect with a wind direction of 315º. Green areas are in the wind shadow.

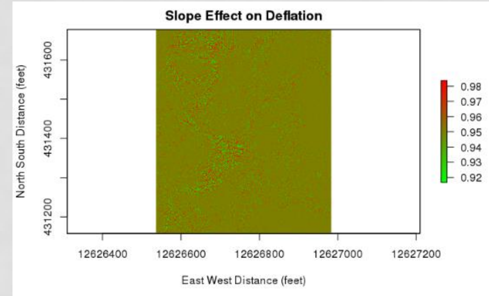

Figure 7: The slope index with a wind direction of 315º.

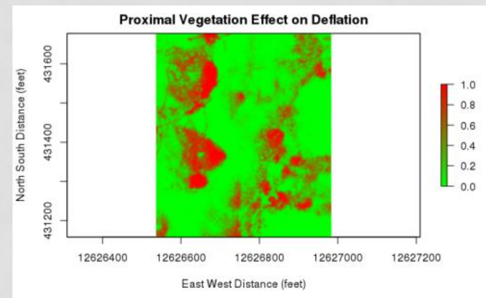

Figure 8: The proximal vegetation index. Note that this is independent of wind direction.

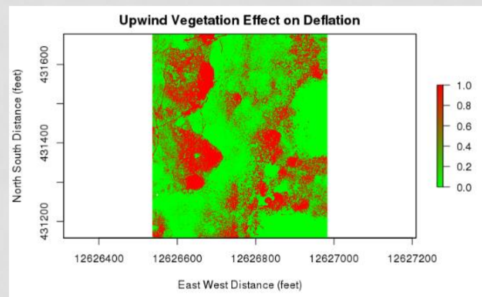

Figure 9: The effect of upwind vegetation with a wind direction of 180º

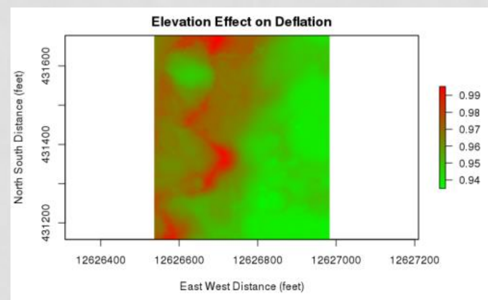

Figure 10: The elevation index of deflation.

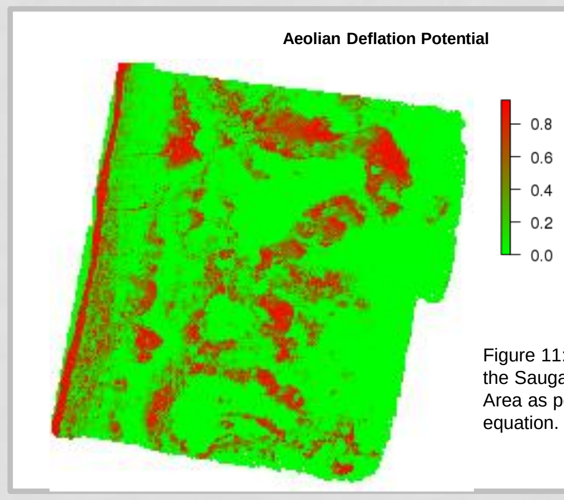

Figure 11: Deflation Potential of the Saugatuck Harbor Natural Area as per the deflation potential equation.

FUTURE WORK

To date, two sets of high-resolution, multispectral images of SHNA have been obtained on drone flights in July, 2017 and July 2018. We plan to collect multispectral images by drone every July for at least the next three years. We will use these images to monitor changes in the proportion, size, orientation, and location of surfaces without vegetation as a proxy of dune mobility. Combined with field observations of sand movement and calculations of wind flow using computational fluid dynamics these will serve to test and refine our predications of sand mobility based on our maps of aeolian deflation potential.

SUMMARY

- Multispectral R-G-B and R-G-NIR high resolution (0.76 cm^2 per pixel) images were acquired during drone flights over a coastal dune complex at Saugatuck Natural Area on the south eastern coast of Lake Michigan.
- The NDVI index was used as a measure of vegetation density in the images.
- A detailed topographic map of the area was obtained using overlapping images from the R-G-B drone flight.
- Topography was combined with vegetation density to make maps showing the calculated values of five indices (wind shadow, slope, elevation, proximal vegetation density and upwind vegetation density) which influence aeolian deflation and dune mobility using the R statistical software package.
- These indices were combined in a simple mathematical model to approximate aeolian deflation potential for winds along the 16 primary directions of the compass rose. These were combined in proportion to the sand drift potential in each directions in a first attempt to create a map of aeolian deflation potential, and hence sensitivity to dune mobility in the study area.
- High-resolution multispectral data will be acquired by drone every July for at least the next three years and will be combined with field studies to test and refine our maps of vegetation density and aeolian deflation potential.

Acknowledgements

- Funding was provided by a Michigan Space Grant Consortium Research Seed Grant (Edward Hansen, Jacob Stid).
- Thanks to Ray David and Jeremy Latchaw at the Mishigami Group for obtaining aerial drone images used in this study.
- This work draws on an earlier study by two undergraduate research students Keri Haddrill in mathematics and Max Huffman in Geology. Ian Gorgenson, another undergraduate research student, calculated the sand drift potentials used in the calculation of aeolian deflation potential.

References

- Fryberger, S. G. 1979. Dune Forms and Wind Regime. In: "A Study of Global Sand Seas", (Ed.): McKee, E. D.. Government Printing Office, Washington, US, pp. 137–160.
- Lancaster, N., and Baas, A., 1998 Influence of vegetation cover on sand transport by wind: field studies at Owens Lake, California. Earth Surface Processes and Landform vol. 23 pp. 69-82.
- NASA, 2017. Measuring Vegetation (NDVI & EVI): Normalized Difference Vegetation Index (NDVI). Web. https://earthobservatory.nasa.gov/Features/ MeasuringVegetation/measuring_vegetation_2.php.
- Pye, K., Blott, S.J., and Howe, M.A., 2014. Coastal Dune Stabilization in Wales and Requirements for Rejuvenation. Journal of Coastal Conservation,18: pp. 27-54.
- Werner, B. 1995. Eolian dunes: Computer simulations and attractor interpretation. Geology vol. 23 pp. 1107-1110.